Stem Cell Reports, Volume *17*

Supplemental Information

Satellite glia of the adult dorsal root ganglia harbor stem cells that yield glia under physiological conditions and neurons in response to injury

Madlyne Maniglier, Marie Vidal, Corinne Bachelin, Cyrille Deboux, Jérémy Chazot, Beatriz Garcia-Diaz, and Anne Baron-Van Evercooren

SUPPLEMENTAL INFORMATION

SUPPLEMENTAL FIGURES AND LEGENDS

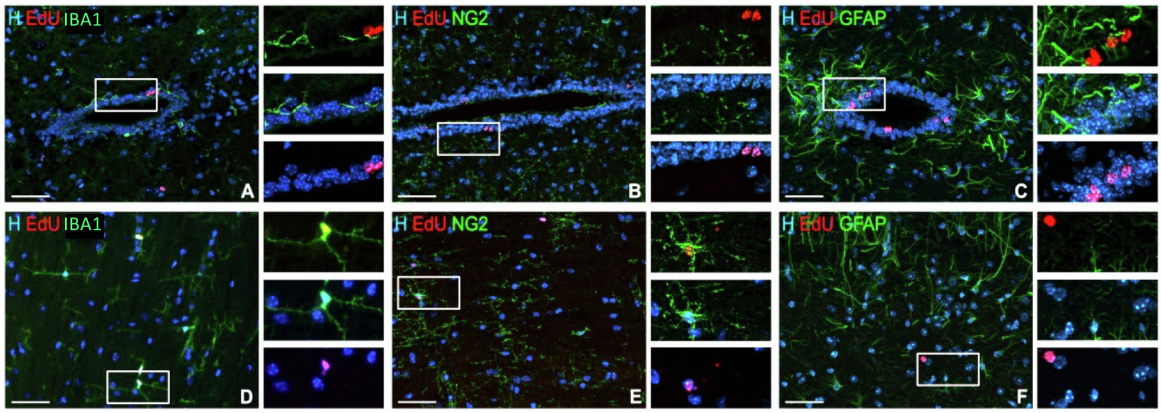

Figure S1 related to Figure 1. ***In Situ characterization of slowly proliferating cells in the adult spinal cord.*** **(A-F)** Double immunohistochemistry for EdU and cell specific markers in the central canal **(A-C)** and parenchyma **(D-F)**. Detection of Iba1+ microglia/macrophages **(A-D)**, NG2+ oligodendrocytes precursors **(B, E)**, GFAP+ glial cells **(C, F)**. Boxed areas are enlarged in right panels. Scale bar: 50 µm.

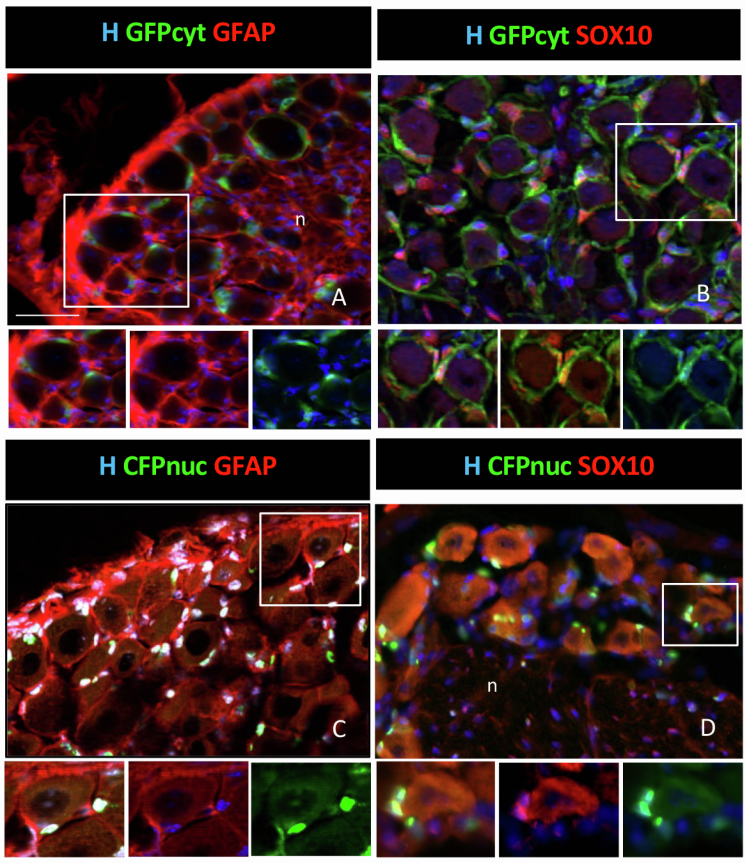

Figure S2 related to Figure 3. **Characterization of DRG-GFPcyt (A, B) and DRG-CFPnuc (C, D) positive cells**. Co-expression with GFAP (**A, C**) or SOX10 (**B, D**). Insets are enlargements of A-D. Scale bar: 50µm

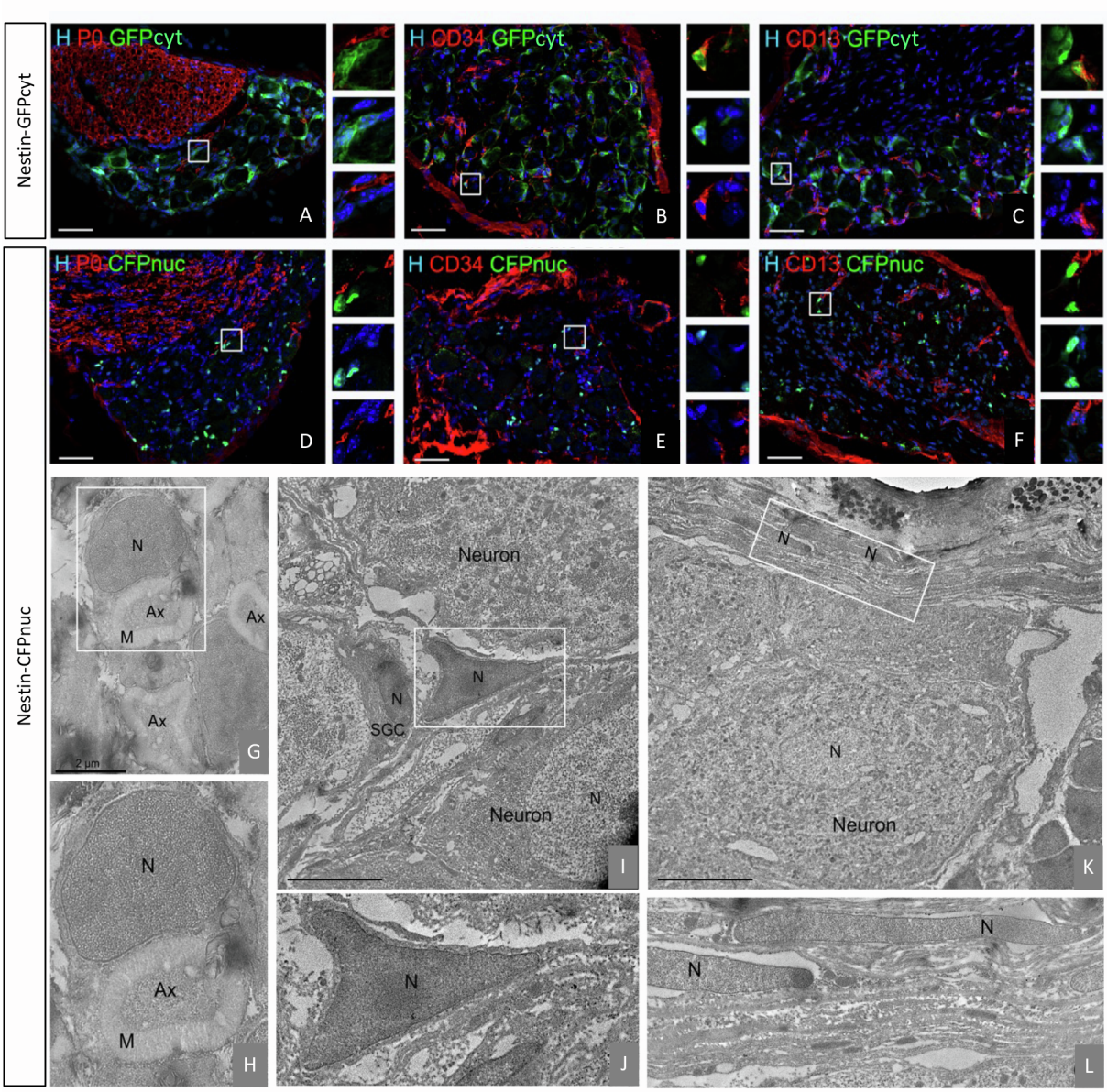

Figure S3 related to Figure 3. ***Characterization of GFPcyt+ or CFPnuc+ cells in the adult DRG of Nestin-GFPcyt and Nestin-CFPnuc reporter mice.*** **(A-F)** Double immunohistochemistry for GFPcyt **(A-C)** or CFPnuc **(D-F)** and cell specific markers to detect P0+ myelinating Schwann cells **(A, D)**, CD34+ endoneurial fibroblasts and endothelial cells **(B, E)** and CD13+ pericytes **(C, F)**. Boxed areas are enlarged in right panels. **(G-L)** Electron microscopy analysis of Nestin-CFPnuc DRG after CFP immunogold labeling. Immunogold particles are never detected in myelinating Schwann cells **(G, H)**, macrophage-like cell **(I, J)** and perineurial fibroblast nuclei **(K, L)**. Lower panels are enlargements of top panels. Scale bar: **A-F**, 50 µm; **G,** 2µm; **I, K,** 5µm**.** A: Axon, M: Myelin, N: Nucleus, SGC: Satellite cell.

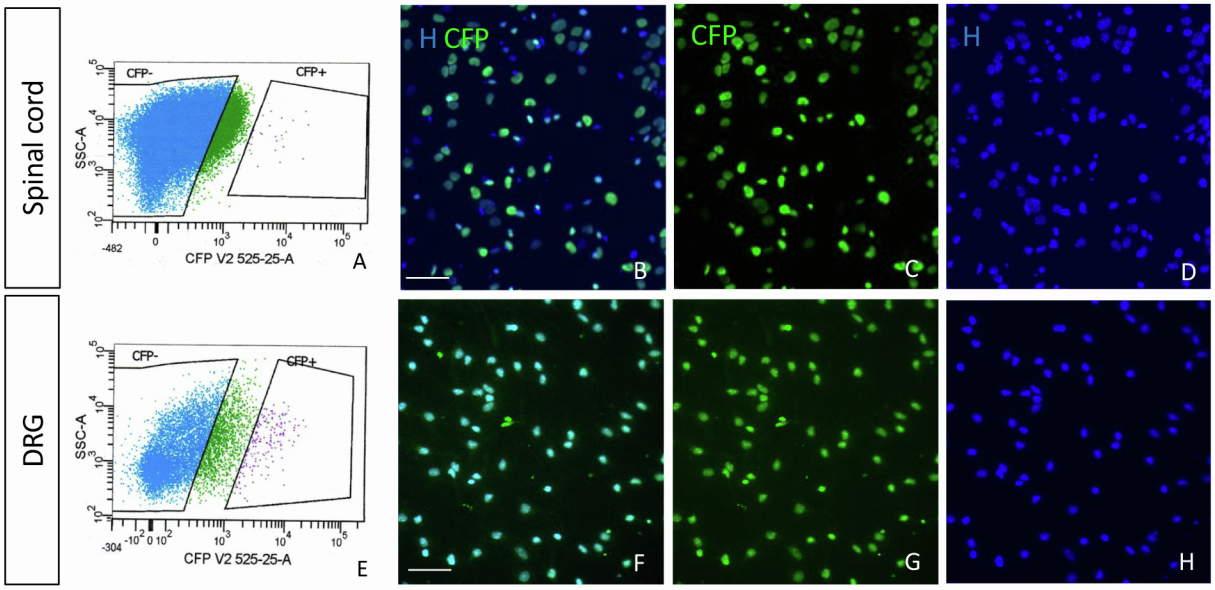

Figure S4 related to Figure 4. ***FACS purification of CFPnuc expressing cells of the spinal cord and DRG***. (**A, E)** FACS gating of CFP+ cells. After sorting cells were allowed to adhere a few hours and were imaged for CFP and Hoechst: (**B, F**) Hoechst and CFP overlay, (**C, G**) CFP expression, (**D, H**) Hoechst expression. Based on Hoechst+ nuclei, around 98% of cells expressed CFP. Scale bar: **B, C, D, F, G, H**, 100µm.

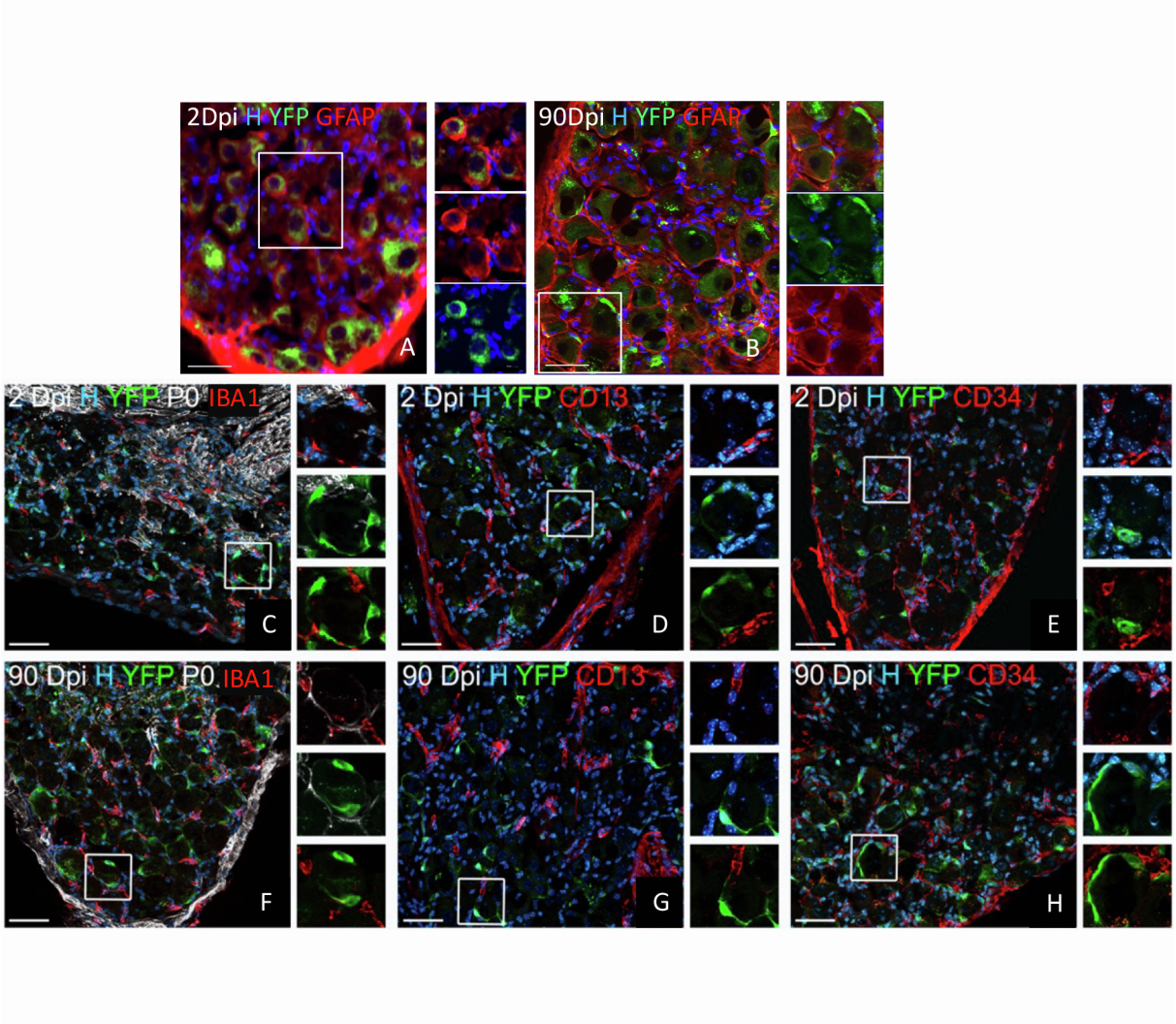

Figure S5 related to Figure 5. ***Characterization of DRG-NSC in non-injured adult Nestin-CreER^{T2}/Rosa26-YFP mice.*** Immunohistochemistry for YFP and cell specific markers to detect co-expression of YFP with **(A, B)** GFAP+ SGC, **(C, F)** P0+ myelinating Schwann cells and Iba1+ microglia/macrophages, **(D, G)** CD13+ pericytes, **(E, H)** CD34+ endoneurial fibroblasts and endothelial cells at 2- and 90 Dpi. Boxed area for each marker is enlarged in the right panel. Scale bar: **A-H**: 50 µm.

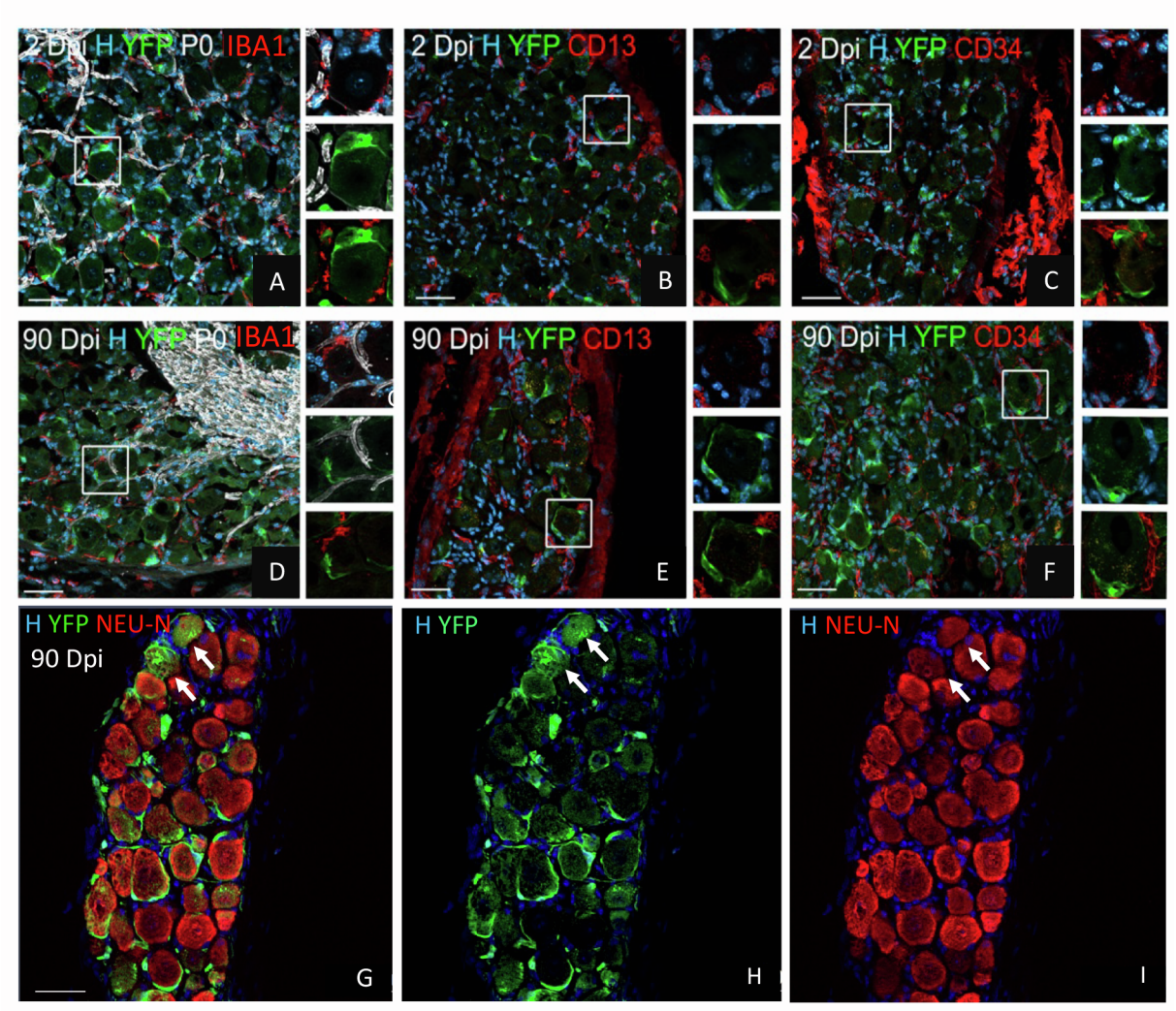

Figure S6 related to Figure 7. ***Characterization of DRG-NSC in injured adult Nestin-CreER^{T2}/Rosa26-YFP mice.*** Immunohistochemistry for YFP and cell type markers to identify Iba1+ microglia/macrophages and P0+ myelinating Schwann cells **(A, D)**, CD13+ pericytes **(B, E)**, and CD34+ endoneurial fibroblasts and endothelial cells **(C, F)** at 2- and 90 Dpi, and YFP+/NEU-N+ neurons at 90Dpi (**G-I**). Boxed area for each marker is enlarged in the right panel. Scale bars: **A-I**: 50μm.

Table S1. List of marker cell specificity for each cell type.

Cell marker	Cell types
IBA1: ionized calcium binding adaptor molecule 1	microglia [1] macrophages[2]
GFAP: glial fibrillary acidic protein	astrocytes[3] stem cells[4] perineuronal satellite glial cells[5]
NG2 glycoprotein	oligodendroglial precursor cells[6] pericytes[7] perineuronal satellite glial cells[8, 9]
SOX10 transcription factor	neural crest cells and their derived progeny including SGC[10, 11]
PV25 parvalbumin	neuronal marker[12, 13]
CD34 transmembrane phospho-glycoprotein protein	endoneurial fibroblasts[14] endothelial cells[15]
CD13 aminopeptidase N	pericytes[16,17]
P0 myelin protein zero	myelinating Schwann cells[18, 19]
CNPase 2′,3′-cyclic nucleotide-3′-phosphodiesterase	oligodendrocytes[20, 21]
MAP2-5 microtubule associated protein 2 and 5	neurons[22, 23]
SMA smooth muscle actin	myofibroblasts[24, 25]
NEU-N Fox-3, Rbfox3, or Hexaribonucleotide Binding Protein-3	neurons[26, 27]
CASPASE 3	apoptotic cells[28, 29]

SUPPLEMENTAL EXPERIMENTAL PROCEDURES

Animals
Nestin CFP-nuclear, Nestin-GFP cytoplasmic, Nestin Cre ERT2, Rosa26-YFP lines were bred and housed under standard conditions of 12-hour light/ 12-hour dark cycles with ad libitum access to dry food and water cycle at ICM pathogen free animal facility. Male and females were included. Experiments were performed according to European Community regulations and INSERM ethical committee (authorization 75-348; 20/04/2005) and were approved by the local Darwin ethical committee.

Sciatic nerve axotomy.
After a resting period of 10 days, tamoxifen-induced animals were anesthetized (Ketamine (100mg/kg) and Xylazin (10mg/kg, Rompun Bayer). In half of the group, the right sciatic nerve was exposed in mid-thigh and cut. A nerve segment of 2 mm was removed to prevent rapid sciatic nerve regeneration. The skin was sutured and mice received two doses of buprenorphin (0.05 mg/kg) in 24 hours. To establish a time course of lesion and re-generation, injured or non-injured induced mice (n= 3-5 per time-point and per group) were sacrificed 2, 14, 30, 60, 90 days dpi. Spinal cord, DRG and sciatic nerves were surgically removed together, in one piece to unambiguously identify the injured DRG (L3-L4-L5), and were processed for immunohistochemistry.

Tissue processing for fluorescent immunohistochemistry.
Four months-old Nestin-CFPnuc and Nestin-GFP-cyt mice (n= 3-4 per line and experimental group) were sacrificed by over-anesthesia (Ketamin-Rompan) and perfused trans-cardially with a solution of 4% paraformaldehyde (PFA) in phosphate saline buffer (PBS) 1X. DRGs, sciatic nerves and spinal cords were post-fixed for one hour in the same fixative, cryo-protected overnight with sucrose 20% in PBS 1X, embedded in Cryomatrix, and frozen in isopentane cooled by liquid nitrogen. Tissues were coronally or horizontally sectioned at 12µm thickness with a cryostat (CM3050S; Leica).

For immunohistochemistry, tissue sections were pre-treated with 0,1 M Glycine for 10 min when needed, followed by incubation in washing buffer (4% bovine serum albumin, BSA) in PBS 1X containing 0.25% Triton) with the following primary antibodies: Chicken anti-GFP (1/300, Aves GFP-1020), mouse anti-NESTIN (1/100, Millipore MAB377), mouse or rabbit anti-GFAP (1/500, Millipore MAB3402 or Dako Z0334), mouse anti-MAP2 (1/200, Sigma M1406), mouse anti-MAP5 (1/200, Sigma M4528, mouse anti-SMA (1/200, Sigma A2547), rabbit anti-NG2 (1/100, Chemicon AB5320), rabbit anti-P75 (1/1000, Millipore AB1554), mouse anti-P0 (Hybridoma[30]), rat anti-CD34 (1/100, BD Biosciences 551387), anti-CASPASE3 (1/400, Cell Signaling), goat anti-SOX10 (1/1000, R&D Systems AF2864), mouse anti-NEU-N (1/100, Millipore MAB377), rabbit NF200 (1/200, Sigma N4142), mouse anti-CNPase (1/200, Millipore MAB326), anti-PDGFRa (1:100, Santa Cruz Biotechnology, sc-338), anti-IBA1 (1:200, Wako, 019-19741), anti-CD-13 (1:50, Biorad MCA2183). After 3 hours, samples were washed three times and incubated for 1 hour with the appropriate fluorochrome-coupled secondary antibodies and Hoechst 33342 (Sigma) diluted in 4% BSA in PBS 1X containing 0.25% Triton. After several rinses in buffer, EdU staining was performed using Click-iT EdU imaging kit (C10340, Invitrogen, Carlsbad, CA) as described in the supplier's protocol. Briefly, slides were incubated with a Click-iT reaction cocktail containing Alexa Fluor 647 azide during 20 min, and washed three times prior mounting in Fluoromount (Sigma). All steps were carried out at room temperature.

Tissue processing for immuno-gold electron microscopy.
Four months-old Nestin-CFP (n=5) mice were sacrificed by overanesthesia (Ketamin-Rompan) and transcardially perfused with 4% PFA in PB 0,1M. DRG and spinal cords were post-fixed one hour in 4% of PFA and 0.3% glutaraldehyde (Sigma-Aldrich). After serial dehydration in a graded ethanol series, tissues were embedded in LRW (Sigma-Aldrich). Post-embedding immunogold was performed incubating ultra-thin sections (80nm) mounted on grids in washing buffer (4% BSA in PB 0.1M) with the primary antibody (chicken anti-GFP antibody, 1/200, Aves GFP-1020). After 1 hour, samples were washed three times and incubated with Goat-anti-Chicken-25nm gold (1/50, Aurion, 125 244). Ultra-thin sections were examined with a HITACHI 120kV HT-7700 transmission electron microscope.

Adult DRG, and spinal cord cultures
Isolation. Transgenic 3 to 4 months-old mice were euthanized by over-anesthesia (CO_2). Spinal cords and DRGs were collected separately into Hank's buffer 1X (HBSS+; Gibco) supplemented with 10%

fetal calf serum (FCS; Gibco) and 1% Penicillin/Streptomycin (P/S; Gibco) and prepared as previously described[31].
Spinal cords were fragmented into 1mm^3 pieces and incubated in DMEM containing 0,05% Trypsin-EDTA (Gibco) and 1% collagenase (Invitrogen) for 30 min at 37°C, then rinsed in stop solution (DMEM plus 10% FCS) and passed through a 40µm cell strainer (BD Biosciences).
DRGs were incubated for 30 min at 37°C, in 0.25% collagenase in DMEM, rinsed in stop solution followed by incubation for 30 min at 37°C, in 0.25% Trypsin. After rinse, DRGs were mechanically dissociated as described above.
Fluorescent Activated Cell Sorting. Cells from the two tissues were purified by FACS, based on their endogenous expression of CFPnuc and GFPcyt (n= 6 independent replicates per transgenic lines).
Expansion. Suspensions of FACS sorted cells were seeded at semi-clonal concentration (<5000 cells/ml) and cultured in suspension as spheres at 37°C/5%CO2 in serum-free medium consisting of DMEM/F12 (1:1; Invitrogen) with B27 and N2 1X (Gibco), 0.8% Insulin (Euromedex), 0,4% glucose, supplemented with epidermal growth factor (EGF, 100ng/mL; Peprotech) and fibroblast growth factor 2 (FGF2, 100ng/mL; Peprotech). Half of the medium was changed every 2-3 days during a period of 10-15 days *in vitro*.
Differentiation. After 15-20 days, spheres were plated on poly-ornithin/laminin (Sigma) coated four well chambers (Greiner) and left in adhesion for 1-2 hours. Adhesive spheres were cultured in the same medium without growth factor for 7-10 days of culture. Cells were fixed in 2% PFA for 10 min prior immunolabeling with the primary and secondary antibodies of interest as described above.

Fluorescence imaging, Quantification and Statistics
Imaging was carried out with an Axio Imager Z2 apotome system (Zeiss) equipped with the Zen software. Images were processed using Adobe Photoshop (Adobe Systems). All quantifications were conducted using the Fiji software. *In vitro* data were deduced from 3-4 experiments performed in duplicates. *In vivo* data were deduced from 5- (for Edu), 10-(for Edu cell type characterization) and 3-(for transgene overlap with other markers) tissue sections from at least 3-4 animals per time-point. Evaluation of EdU expression *in situ* was based on the degree (%) of overlap of EdU- and Hoechst stainings with low <33%, medium <66% and high>66% overlap respectively. Quantification of newly-born neurons (NEU-N+/YFP+) after injury was performed screening 3 DRG- and an average of 700 Neurons- and 625 YFP+ cells/mouse (n=3) and was based on Z stacks images and considering only cells with full overlap of YFP and NEU-N positivities.
Statistical analysis was carried out using GraphPad Prism 6 software. All values were expressed as mean ± SD. Normality in the variable distributions was assessed by the D'Agostino&Pearson omnibus test and Grubbs' test was used to detect and exclude possible outliers. When Normality test was passed, means were compared by two-tailed Student's t test. When one or both groups did not follow a normal distribution, means were compared by two-tailed Mann-Whitney U test. When different independent groups were compared, we performed a one-way or two-way ANOVA plus Dunnett's test or Tukey's multiple comparison tests as specify in each experiment. P-values lower than 0.05 were used as a cut-off for statistical significance.

SUPPLEMENTAL REFERENCES

1. Ohsawa, K., Imai, Y., Sasaki, Y., and Kohsaka, S. (2004). Microglia/macrophage-specific protein Iba1 binds to fimbrin and enhances its actin-bundling activity. J Neurochem *88*, 844-856. 10.1046/j.1471-4159.2003.02213.
2. Kenkhuis, B., Somarakis, A., Kleindouwel, L.R.T., van Roon-Mom, W.M.C., Hollt, T., and van der Weerd, L. (2022). Co-expression patterns of microglia markers Iba1, TMEM119 and P2RY12 in Alzheimer's disease. Neurobiol Dis *167*, 105684. 10.1016/j.nbd.2022.105684
3. Yang, Z., and Wang, K.K. (2015). Glial fibrillary acidic protein: from intermediate filament assembly and gliosis to neurobiomarker. Trends Neurosci *38*, 364-374. 10.1016/j.tins.2015.04.003
4. Liu, Y., Namba, T., Liu, J., Suzuki, R., Shioda, S., and Seki, T. (2010). Glial fibrillary acidic protein-expressing neural progenitors give rise to immature neurons via early intermediate progenitors expressing both glial fibrillary acidic protein and neuronal markers in the adult hippocampus. Neuroscience *166*, 241-251. 10.1016/j.neuroscience.2009.12.026
5. Mohr, K.M., Pallesen, L.T., Richner, M., and Vaegter, C.B. (2021). Discrepancy in the Usage of GFAP as a Marker of Satellite Glial Cell Reactivity. Biomedicines *9*. 10.3390/biomedicines9081022

6. Karram, K., Chatterjee, N., and Trotter, J. (2005). NG2-expressing cells in the nervous system: role of the proteoglycan in migration and glial-neuron interaction. J Anat *207*, 735-744. 10.1111/j.1469-7580.2005.00461.
7. Ozerdem, U., Monosov, E., and Stallcup, W.B. (2002). NG2 proteoglycan expression by pericytes in pathological microvasculature. Microvasc Res *63*, 129-134. 10.1006/mvre.2001.2376
8. Rezajooi, K., Pavlides, M., Winterbottom, J., Stallcup, W.B., Hamlyn, P.J., Lieberman, A.R., and Anderson, P.N. (2004). NG2 proteoglycan expression in the peripheral nervous system: upregulation following injury and comparison with CNS lesions. Mol Cell Neurosci *25*, 572-584. 10.1016/j.mcn.2003.10.009
9. Huang, B., Zdora, I., de Buhr, N., Lehmbecker, A., Baumgartner, W., and Leitzen, E. (2021). Phenotypical peculiarities and species-specific differences of canine and murine satellite glial cells of spinal ganglia. J Cell Mol Med *25*, 6909-6924. 10.1111/jcmm.16701
10. Britsch, S., Goerich, D.E., Riethmacher, D., Peirano, R.I., Rossner, M., Nave, K.A., Birchmeier, C., and Wegner, M. (2001). The transcription factor Sox10 is a key regulator of peripheral glial development. Genes Dev *15*, 66-78. 10.1101/gad.186601
11. Wahlbuhl, M., Reiprich, S., Vogl, M.R., Bosl, M.R., and Wegner, M. (2012). Transcription factor Sox10 orchestrates activity of a neural crest-specific enhancer in the vicinity of its gene. Nucleic Acids Res *40*, 88-101. 10.1093/nar/gkr734
12. Dorst, M.C., Diaz-Moreno, M., Dias, D.O., Guimaraes, E.L., Holl, D., Kalkitsas, J., Silberberg, G., and Goritz, C. (2021). Astrocyte-derived neurons provide excitatory input to the adult striatal circuitry. Proc Natl Acad Sci U S A *118*. 10.1073/pnas.2104119118
13. Filice, F., Vorckel, K.J., Sungur, A.O., Wohr, M., and Schwaller, B. (2016). Reduction in parvalbumin expression not loss of the parvalbumin-expressing GABA interneuron subpopulation in genetic parvalbumin and shank mouse models of autism. Mol Brain *9*, 10. 10.1186/s13041-016-0192-8
14. Hirose, T., Tani, T., Shimada, T., Ishizawa, K., Shimada, S., and Sano, T. (2003). Immunohistochemical demonstration of EMA/Glut1-positive perineurial cells and CD34-positive fibroblastic cells in peripheral nerve sheath tumors. Mod Pathol *16*, 293-298. 10.1097/01.MP.0000062654.83617.B7
15. Richard, L., Topilko, P., Magy, L., Decouvelaere, A.V., Charnay, P., Funalot, B., and Vallat, J.M. (2012). Endoneurial fibroblast-like cells. J Neuropathol Exp Neurol *71*, 938-947. 10.1097/NEN.0b013e318270a941
16. Smyth, L.C.D., Rustenhoven, J., Scotter, E.L., Schweder, P., Faull, R.L.M., Park, T.I.H., and Dragunow, M. (2018). Markers for human brain pericytes and smooth muscle cells. J Chem Neuroanat *92*, 48-60. 10.1016/j.jchemneu.2018.06.001
17. Crouch, E.E., and Doetsch, F. (2018). FACS isolation of endothelial cells and pericytes from mouse brain microregions. Nat Protoc *13*, 738-751. 10.1038/nprot.2017.158
18. Nagarajan, R., Le, N., Mahoney, H., Araki, T., and Milbrandt, J. (2002). Deciphering peripheral nerve myelination by using Schwann cell expression profiling. Proc Natl Acad Sci U S A *99*, 8998-9003. 10.1073/pnas.132080999
19. Jessen, K.R., and Mirsky, R. (2019). Schwann Cell Precursors; Multipotent Glial Cells in Embryonic Nerves. Front Mol Neurosci *12*, 69. 10.3389/fnmol.2019.00069
20. Verrier, J.D., Jackson, T.C., Gillespie, D.G., Janesko-Feldman, K., Bansal, R., Goebbels, S., Nave, K.A., Kochanek, P.M., and Jackson, E.K. (2013). Role of CNPase in the oligodendrocytic extracellular 2',3'-cAMP-adenosine pathway. Glia *61*, 1595-1606. 10.1002/glia.22523
21. Soltani, M.H., Pichardo, R., Song, Z., Sangha, N., Camacho, F., Satyamoorthy, K., Sangueza, O.P., and Setaluri, V. (2005). Microtubule-associated protein 2, a marker of neuronal differentiation, induces mitotic defects, inhibits growth of melanoma cells, and predicts metastatic potential of cutaneous melanoma. Am J Pathol *166*, 1841-1850. 10.1016/S0002-9440(10)62493-5
22. Cheng, A., Krueger, B.K., and Bambrick, L.L. (1999). MAP5 expression in proliferating neuroblasts. Brain Res Dev Brain Res *113*, 107-113. 10.1016/s0165-3806(99)00006-1
23. Hinz, B., Dugina, V., Ballestrem, C., Wehrle-Haller, B., and Chaponnier, C. (2003). Alpha-smooth muscle actin is crucial for focal adhesion maturation in myofibroblasts. Mol Biol Cell *14*, 2508-2519. 10.1091/mbc.e02-11-0729
24. Ina, K., Kitamura, H., Tatsukawa, S., and Fujikura, Y. (2011). Significance of alpha-SMA in myofibroblasts emerging in renal tubulointerstitial fibrosis. Histol Histopathol *26*, 855-866. 10.14670/HH-26.855
25. Wolf, H.K., Buslei, R., Schmidt-Kastner, R., Schmidt-Kastner, P.K., Pietsch, T., Wiestler, O.D., and Blumcke, I. (1996). NeuN: a useful neuronal marker for diagnostic histopathology. J Histochem Cytochem *44*, 1167-1171. 10.1177/44.10.8813082

26. Duan, W., Zhang, Y.P., Hou, Z., Huang, C., Zhu, H., Zhang, C.Q., and Yin, Q. (2016). Novel Insights into NeuN: from Neuronal Marker to Splicing Regulator. Mol Neurobiol *53*, 1637-1647. 10.1007/s12035-015-9122-5
27. Crowley, L.C., and Waterhouse, N.J. (2016). Detecting Cleaved Caspase-3 in Apoptotic Cells by Flow Cytometry. Cold Spring Harb Protoc *2016*. 10.1101/pdb.prot087312
28. Porter, A.G., and Janicke, R.U. (1999). Emerging roles of caspase-3 in apoptosis. Cell Death Differ *6*, 99-104. 10.1038/sj.cdd.4400476
29. Michalski, D., Keck, A.L., Grosche, J., Martens, H., and Hartig, W. (2018). Immunosignals of Oligodendrocyte Markers and Myelin-Associated Proteins Are Critically Affected after Experimental Stroke in Wild-Type and Alzheimer Modeling Mice of Different Ages. Front Cell Neurosci *12*, 23. 10.3389/fncel.2018.00023
30. Yoshimura, T., Satake, M., Kobayashi ,T., (1996) Connexin43 is another gap junction protein in the peripheral nervous system. J Neurochem 1996 Sep;67(3):1252-8
31. Vidal, M., Maniglier, M., Deboux, C., Bachelin, C., Zujovic, V. and Baron-Van Evercooren, A. (2015). Adult DRG stem/progenitor cells generate pericytes in the presence of central nervous system (CNS) developmental cues, and Schwann cells in response to CNS demyelination. *Stem Cells* 33, 2011–24.